A novel method for simulating quantum dissipative systems

Jianshu Cao, Lowell W. Ungar, and Gregory A. Voth
Department of Chemistry, University of Pennsylvania, Philadelphia, Pennsylvania 19104-6323

(Received 27 July 1995; accepted 15 December 1995)

An effective and flexible numerical scheme is proposed to simulate the dissipative quantum dynamics of a linearized system–bath Hamiltonian. Based on the observation that the Feynman path integrals for a Gaussian bath have a quadratic functional form, the bath average can be performed by directly sampling paths of the discretized harmonic modes and then propagating the system under the influence of quantum Gaussian force. The algorithm is amenable to all known quantum propagation methods and can thus be flexibly applied to study quantum dissipation in the condensed phase. Nontrivial numerical examples based on the spin-boson and damped quantum oscillator models are presented to demonstrate the application of the new algorithm. © *1996 American Institute of Physics.* [S0021-9606(96)51011-4]

I. INTRODUCTION

One of the most challenging problems in physics and chemistry is the dynamical simulation of quantum dissipative systems.[1–7] Quantum dissipation arises from the coupling of a quantum system to a ''bath'' which consists of an infinite number of degrees of freedom. This results in a time irreversible dynamics of the system. Most accurate methods for quantum simulation such as basis set expansions have been limited to a few degrees of freedom and/or short time dynamics, thus being incapable of treating dissipation. On the other hand, the recently developed *centroid molecular dynamics* (CMD) method allows one to simulate the dynamics of a general quantum many-body system approximately.[8–16] Although the latter approach is a significant step forward, an accurate and general numerical algorithm for *exactly* simulating quantum dynamics in condensed phases is not yet available now nor is one expected in the near future due to the fundamental numerical complexity of the problem. By necessity therefore (and often with some justification!), the focus often turns to the linearized quantum dissipation model, sometimes termed the *Gaussian bath model* (see, e.g., Refs. 17–20). The latter has become the subject of many analytical and numerical studies, as well as a model for several *real* condensed phase dynamical processes such as activated dynamics, electron and proton transfer, vibrational energy relaxation, diffusion, etc. Within the context of this important model, it is the focus of the present paper to propose a simple and powerful algorithm to simulate the dynamics of quantum systems linearly coupled to a Gaussian bath.

The Gaussian bath model consists of one or more system degrees of freedom q coupled to N linear bath harmonic oscillators $\{x_i\}$ as described by the potential

$$V=V_{\mathrm{eq}}(q)+\sum_{i=1}^{N}\frac{1}{2}m_i\omega_i^2\left(x_i-\frac{c_i}{m_i\omega_i^2}q\right)^2, \tag{1.1}$$

where $V_{\mathrm{eq}}(q)$ is the potential of mean force along q, x_i is the ith Gaussian bath normal mode, m_i is the mass, ω_i is the harmonic frequency, and c_i is the coupling strength. It was shown by Zwanzig[17] that the elimination of the bath modes from the classical equations of motion for the above potential yields the generalized Langevin equation (GLE),

$$m\ddot{q}(t)+\frac{d}{dq}V_{\mathrm{eq}}[q(t)]+\int_0^t dt'\,\eta(t-t')\dot{q}(t')=F(t), \tag{1.2}$$

where $F(t)$ is the random force and m is the effective mass of the coordinate q. The dynamical friction kernel $\eta(t)$ is then identified as

$$\eta(t)=\sum_{i=1}^{N}\frac{c_i^2}{m_i\omega_i^2}\cos(\omega_i t)=\frac{2}{\pi}\int_0^\infty\frac{d\omega}{\omega}J(\omega)\cos(\omega t), \tag{1.3}$$

where $J(\omega)$ is the spectral density, defined in the discrete bath limit by

$$J(\omega)=\frac{\pi}{2}\sum_{i=1}^{N}\frac{c_i^2}{m_i\omega_i}\delta(\omega-\omega_i). \tag{1.4}$$

The random force can be explicitly expressed in terms of the initial conditions of the bath variables. Therefore, under the assumption that the initial bath distribution in phase space is in thermal equilibrium in the presence of the system, one can readily show that

$$\eta(t)=\beta\langle F(t)F(0)\rangle_{\mathrm{bath}}, \tag{1.5}$$

where the equilibrium condition $\langle F\rangle_{\mathrm{bath}}=0$ is implied. The introduction of the spectral density $J(\omega)$ makes it possible to pass from a discrete set of modes to a continuum spectrum, and hence to represent an arbitrary time dependent friction $\eta(t)$. The relation in Eq. (1.5) holds for a Gaussian bath regardless of the form of the potential of mean force. It is for this reason that the Gaussian bath is an attractive analytical model to study the solvent frictional effects on, e.g., vibrational relaxation and activated reaction dynamics.

The Gaussian bath can, in principle, be easily quantized to represent quantum dissipation and thereby can serve as a prototype for formulating quantum Brownian motion, dissipative tunneling, solvent-induced electron transfer and other quantum processes in the condensed phase. Note that the system variable q can represent a single- or multidimensional vector or a discretized variable such as a complete set of eigenstates, though it is written as a scalar in Eq. (1.2). Integration over the bath modes in the path integral formulation leads to an influence functional which couples different time slices of the Feynman paths of the system variable.[1,21] Coalson[22,23] and Mak and co-workers[24–27] have presented a series of studies of the spin-boson model,[28] by real time Monte Carlo methods. Makri and co-workers have also developed the quasiadiabatic propagator path integral methods (QUAPI) which propagate a one-dimensional system adiabatically while the influence functional is incorporated by coupling a finite number of neighboring time slices.[29–33] By virtue of this algorithm and discrete variable representation (DVR) quadrature, they recently presented, for example, a detailed numerical study of quantum activated rates for a double well coupled to a harmonic bath in order to compare with the results of several approximate theories.[31] However, both approaches are based on the influence functional formulation which, while very intuitive and powerful, may not be the optimal choice for wavefunction propagation or semiclassical approximations.

In this paper, we will develop a simple algorithm to sample the Gaussian force directly without making use of the influence functional formalism, thus presenting an alternative algorithm which appears to be more flexible and general. The new algorithm is described in Sec. II and some examples are demonstrated in Sec. III, including the spin-boson model and the dissipative quantum oscillator. The latter study also provides a comparison with CMD. Concluding remarks are given in Sec. IV.

II. DIRECT SAMPLING OF THE GAUSSIAN FORCE

To begin, the Hamiltonian is written as

$$H=H_q(q)+H_b(x)+V_c(x,q), \tag{2.1}$$

where $H_b(x)$ is the "bath" Hamiltonian given by

$$H_b=\sum_{i=1}^{N}\left(\frac{p_i^2}{2m_i}+\frac{1}{2}\,m_i\omega_i^2x_i^2\right), \tag{2.2}$$

$H_q(q)$ is the "system" part of the Hamiltonian, and $V_c(x,q)$ is the coupling potential. In principle, $V_c(x,q)$ can take any form, but for the method described in this paper, numerical difficulties increase with the nonlinearity in the coupling potential. If the quantity of interest, F, is a function of the system variables only, then one can express this quantity at time t in terms of a bath path average, defined as

$$\langle F[x_f(t'),x_b(t'),x_\beta(\tau)]\rangle_{\text{bath}}\,\frac{\int dx_1\int dx_2\int dx_3\int\mathscr{D}x_f(t')\int\mathscr{D}x_b(t')\int\mathscr{D}x_\beta(\tau)F[x_f(t'),x_b(t'),x(\tau)]\exp(-\bar{S}/\hbar)}{\int dx_1\int dx_2\int dx_3\int\mathscr{D}x_f(t')\int\mathscr{D}x_b(t')\int\mathscr{D}x_\beta(\tau)\exp(-\bar{S}/\hbar)}, \tag{2.3}$$

where $x_f(t')$ is the real time forward path satisfying the boundary conditions $x_f(0)=x_1$ and $x_f(t)=x_3$, $x_b(t')$ is the backward real time path satisfying the boundary conditions $x_b(0)=x_2$ and $x_b(t)=x_3$, and $x_\beta(\tau)$ is the imaginary time path satisfying the boundary conditions $x_\beta(0)=x_1$ and $x_\beta(\hbar\beta)=x_2$, so that a closed trace path is formed for the thermal averaged real time propagation for $t'=0$ to $t'=t$ at temperature $\beta=1/k_BT$. Here, $\bar{S}$ is the summation of real and imaginary time action functionals[1,21] for the pure bath (H_b), evaluated along the closed path. It is explicitly given by

$$\bar{S}=S_\beta[x_\beta(\tau)]-iS[x_f(t')]+iS[x_b(t')], \tag{2.4}$$

where $S[x_f(t')]$ is the real time action functional[1] for the forward path, $S[x_b(t')]$ is the real time action functional for the backward path, and $S_\beta[x(\tau)]$ is the imaginary time action functional.[21] With the introduction of the bath average, the formal expression of a physical quantity of the system can be simplified. For example, a time correlation function is expressed as

$$\langle A(t)B(0)\rangle =\frac{\langle \mathrm{Tr}[e^{i\int_0^t dt'H(t')/\hbar}Ae^{-i\int_0^t dt'H(t')/\hbar}Be^{-\int_0^{\beta\hbar}d\tau H(\tau)/\hbar}]\rangle_{\text{bath}}}{\langle \mathrm{Tr}[e^{i\int_0^t dt'H(t')/\hbar}e^{-i\int_0^t dt'H(t')/\hbar}e^{-\int_0^{\beta\hbar}d\tau H(\tau)/\hbar}]\rangle_{\text{bath}}}, \tag{2.5}$$

where operators A and B are evaluated at the final time t and the initial time 0, respectively. In the above equation, $H(t')=H_q(q)+V_c[x(t'),q]$ is the time-dependent system Hamiltonian evolving under the influence of the Gaussian bath, the Tr symbol denotes a trace over the system variables, and the exponentiated operators are understood as being time-ordered products.

Our approach is based on a simple idea. Since the bath actions are quadratic and thus the functional integrand of Eq. (2.3) in the discretized form is a multidimensional complex Gaussian function, the bath average can be performed by direct Monte Carlo sampling. Given a bath path generated by the Gaussians, the system can be propagated under the influence of the time-dependent fluctuating bath force through any method of choice, such as matrix or tensor multiplication,[31,34] split operator propagation,[35] wave packet dynamics,[36] semiclassical propagator,[3,37,38] CMD,[8–11] etc. Averaging the time-dependent system quantities over the bath variables yields the desired physical quantities of the overall quantum system–bath Hamiltonian. This procedure clearly points to a very large array of possibilities for computing the quantum dynamical evolution of such systems. The present Gaussian force method is to be contrasted with a method developed by Coalson[22] wherein the harmonic bath evolution is calculated under the time dependent influence of quantum spin system paths, assuming the coupling is linear in the bath coordinates.

The first step towards our goal is to sample the three terminal points on the trace loop described by the quadratic action

$$
\begin{aligned}
S(x_1,x_2,x_3)/\hbar &= [S_\beta(x_1,x_2,\hbar\beta) - iS_f(x_1,x_3,t) + iS_b(x_2,x_3,t)]/\hbar \\
&= \frac{m\omega}{2\hbar\ \sinh(\hbar\beta\omega)}\,[(x_1^2+x_2^2)\cosh(\hbar\beta\omega) - 2x_1x_2] \\
&\quad - i\,\frac{m\omega}{2\hbar\ \sin(\omega t)}\,[(x_1^2+x_3^2)\cos(\omega t) - 2x_1x_3] \\
&\quad + i\,\frac{m\omega}{2\hbar\ \sin(\omega t)}\,[(x_2^2+x_3^2)\cos(\omega t) - 2x_2x_3] \\
&= \frac{1}{2}\,\mathbf{x}^\dagger(\mathbf{S}/\hbar)\mathbf{x},
\end{aligned} \tag{2.6}
$$

where $\mathbf{x}=(x_1,x_2,x_3)$ is a three-dimensional vector and $\mathbf{S}/\hbar$ is a 3×3 matrix. Hereafter in this section, a single Gaussian bath mode notation is adopted for simplicity unless specified otherwise. It is shown in the Appendix that the three-dimensional complex matrix $\mathbf{S}/\hbar$ can be diagonalized by a transformation matrix $\mathbf{U}$ such that

$$
\exp(-S/\hbar) = \exp[-(\lambda_1 y_1^2 + \lambda_2 y_2^2 + \lambda_3 y_3^2)/2], \tag{2.7}
$$

where $\mathbf{y}$ is the transformed terminal coordinates, determined by $\mathbf{y}=\mathbf{U}^{-1}\mathbf{x}$, and $\{\lambda\}$ are the elements of the diagonalized matrix $\mathbf{S}/\hbar$. Expressions for both $\mathbf{U}$ and $\{\lambda\}$ are given in the Appendix.

It should be noted that both the transformation matrix $\mathbf{U}$ and the resultant $\{\lambda\}$ are complex functions. In order to perform the Monte Carlo sampling with a complex Gaussian function $e^{-\lambda y^2/2}$, one introduces a coordinate rotation, given by

$$
\eta = y\ \exp(i\theta/2), \tag{2.8}
$$

where the rotation angle θ is determined from the relation $\lambda=\rho e^{i\theta}$, so that the rotated Gaussian function reads

$$
\exp(-\lambda y^2/2) = \exp(-\rho\eta^2/2). \tag{2.9}
$$

Then, any average value of a function of y can be expressed as

$$
\begin{aligned}
\langle f(y)\rangle_\lambda &= \sqrt{\frac{\lambda}{2\pi}}\int_{-\infty}^{\infty} dy f(y) e^{-\lambda y^2/2} \\
&= \sqrt{\frac{\rho}{2\pi}}\int_{-\infty}^{\infty} d\eta f(\eta e^{-i\theta/2}) e^{-\rho\eta^2/2}.
\end{aligned} \tag{2.10}
$$

This procedure thus removes the sign problem of any quadratic actions in the Monte Carlo sampling. Similar coordinate rotations to enable real time Gaussian sampling have been employed by Doll *et al.*[39] and by Chang and Miller.[40]

The overall transformation from an average over real $\mathbf{x}$ to an average over real $\boldsymbol{\eta}$ requires a rotation of the integration region that is valid if the averaged function contains no singularities between the initial and final surfaces. The complex Gaussian $\exp(-S/\hbar)$ is easily shown to be finite for all real $\mathbf{x}$, all real $\boldsymbol{\eta}$, and in between. The exponent of $V_c(t)$ cannot then cause singularities if the coupling is linear in the bath coordinates—but under other conditions the validity of the transformation must be established.

The next step is to sample the intermediate time slices of the discretized Feynman paths. Given the two end points x_t and x_0 of the bath paths as specified by the boundary conditions of the bath path integration, one has the real time propagator in the discretized form[1]

$$
\begin{aligned}
\langle x_t | e^{-iH_b t/\hbar} | x_0\rangle &= \left[\frac{m\omega}{2\pi i\hbar\ \sin(\omega t)}\right]^{P/2} \\
&\quad \times \prod_{n=1}^{P} \int dx_n \exp\Bigg\{ i\,\frac{m\omega}{2\hbar\ \sin(\omega\epsilon)} \\
&\quad \times \sum_{n=1}^{P} [(x_{n-1}^2 + x_n^2)\cos(\omega\epsilon) - 2x_{n-1}x_n]\Bigg\},
\end{aligned} \tag{2.11}
$$

where the subscripts denote the discretized time slice of increment $\epsilon=t/P$ and $x_P=x_t$. Introducing the classical trajectory $x_{\rm cl}(t')$ and the discretized Fourier modes a_l, one can then Fourier decompose the path as

$$
x_n = x_{\rm cl}(t_n) + \sum_{l=1}^{P-1} a_l\ \sin(l\pi n/P), \tag{2.12}
$$

where the classical solution connecting the two end points is given by

$$
x_{\rm cl}(t') = \frac{x_t\ \sin(\omega t') + x_0\ \sin[\omega(t-t')]}{\sin(\omega t)} \tag{2.13}
$$

and the Fourier modes diagonalize the quadratic action functional. Consequently, the real time action functional assumes the form

$$
\begin{aligned}
S([x_n]) &= S_f(x_0,x_t;t) \\
&\quad + \sum_{l=1}^{P-1} \frac{m\bar{t}}{2\hbar}\left\{2[1-\cos(\pi l/P)]\,\frac{P^2}{\bar{t}^2} - \bar{\omega}^2\right\} a_l^2/2.
\end{aligned} \tag{2.14}
$$

Here, because of the use of the exact quadratic propagator, the parameters $\bar{t}$ and $\bar{\omega}$ are the rescaled time and frequency, defined by

$$
\begin{aligned}
\bar{t} &= t\ \frac{\sin(R)}{R}, \\
\bar{\omega} &= \omega\ \frac{1}{\cos(R/2)},
\end{aligned} \tag{2.15}
$$

with $R=\omega t/P$. Again, the coordinate rotation for the Fourier modes $\{a_n\}$ is employed to treat the complex Gaussian functions, with the same condition of lack of singularities in the rotation that was discussed previously. A similar procedure can be applied to the backward real time paths and, in imaginary time, to the thermal paths.

With the above two steps in hand, one can simulate the dynamics of the quantum subsystem interacting with the Gaussian bath. The procedure is described as follows:

(a) Choose a finite set of linear harmonic oscillators to represent the Gaussian bath. Care must be taken to avoid nonergodicity of the bath for the time period of interest (i.e., a large enough set of bath oscillators must be chosen to adequately represent the continuum spectral density function *as it affects the system dynamics*).

(b) For each bath mode, sample the three terminal points according to the distribution in Eq. (2.7) and generate a realization of the forward, backward, and imaginary time bath paths according to the distribution based on the Fourier path modes [cf. Eq. (2.14)]. If the coupling is linear, the quantum fluctuating force is the superposition of the contributions from all the modes and can be obtained in the time domain using fast Fourier transform methods.[39]

(c) The quantum system, defined for the coordinate(s) q, is then propagated by whatever means is desirable under the influence of the time-dependent complex quantum force, and the quantity of interest is computed [cf. Eqs. (2.3) and (2.5)]. Because of the force, the effective system Hamiltonian is time dependent and may be non-Hermitian.

(d) Steps (b) and (c) are then repeated for many independent bath configurations. The bath-averaged dynamical quantity represents the dynamical evolution of the quantum system under the influence of the dissipative environment.

III. REPRESENTATIVE APPLICATIONS

A. Spin-boson model

Although the formulation of the previous section is general, we will carry out calculations for the spin-boson model in order to test the accuracy and feasibility of the proposed algorithm. In spite of its apparent simplicity, the spin-boson Hamiltonian serves as the primary model for investigating nonadiabatic transitions because of its physical richness (see, e.g., Ref. 28). To specialize the method to treat the spin-boson model, q now represents a discrete spin operator and the coupling potential V_c in Eq. (2.1) becomes bilinear. The resulting Hamiltonian for the spin-boson model is thus given as

$$H=\Delta\sigma_x+\sum_{i=1}^{N}\left[\frac{1}{2}\,m_i\dot{x}_i^2+\frac{1}{2}\,m_i\omega_i^2\left(x_i-\frac{c_i}{m_i\omega_i^2}\,\sigma_z\right)^2\right], \tag{3.1}$$

where σ is the Pauli spin matrix, Δ is one-half the bare tunnel splitting, and the modes $\{x\}$ constitute the Gaussian bath. The parameters are chosen in the present case to be $\hbar=1.0$, $\Delta=0.8$, $m=1.0$. The parameters of the bath were chosen so that its spectral density, given in discrete form by Eq. (1.4), reproduces an appropriate friction kernel in the classical limit.

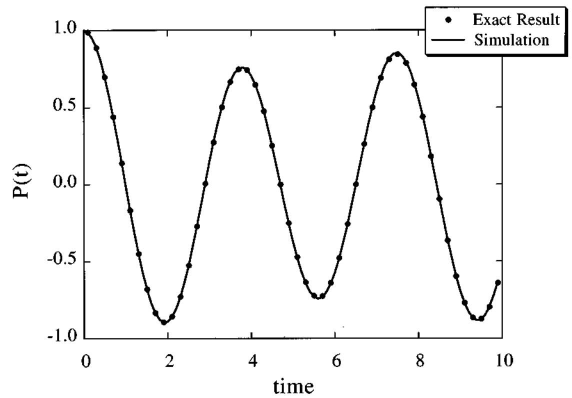

FIG. 1. A plot of $P(t)$ for a spin system coupled to a single bath mode as described in the text. The exact results (represented by solid circles) were obtained from a basis-set calculation.

The physical quantity for this study is a population distribution function, $P(t)$, which is the population difference between the up-spin state and the down-spin state, assuming only the up-spin state is occupied initially. In terms of correlation functions, $P(t)$ can be explicitly expressed as[41]

$$P(t)=\frac{\langle\sigma_{\rm up}(0)\sigma_z(t)\sigma_{\rm up}(0)\rangle}{\langle\sigma_{\rm up}\rangle}, \tag{3.2}$$

where $\sigma_{\rm up}$ projects out the up-spin state,

$$\sigma_{\rm up}=\begin{pmatrix}1 & 0\\ 0 & 0\end{pmatrix}. \tag{3.3}$$

Because of the simplicity of the spin matrix, the spin system can be propagated by diagonalizing the short-time propagator. Therefore, the nondissipative spin dynamics is accurate and the dissipative spin dynamics is accurate to order δt^3 with a proper operator splitting.[42] In all the simulations, between 10^4 and 10^5 independent Gaussian bath configurations were sampled to achieve a statistically converged bath average.

To test the new algorithm, the case of a single mode bath was first considered. That is, the Gaussian bath consisted of only one harmonic oscillator with $\omega=1.0$ and $c=0.2$. In Fig. 1 the population difference $P(t)$ is shown as a function of time and is compared with the exact results obtained from a basis set calculation.

The calculations next focused on the case of a continuous bath. To represent the continuous limit of the spectral density in Eq. (1.4), the spectrum was discretized evenly up to a chosen cutoff frequency. The coupling coefficients c_i for the discrete bath were chosen according to the formula

$$c_i^2=\frac{2}{\pi}\,m\omega_i J(\omega_i)\Delta\omega, \tag{3.4}$$

where $\Delta\omega$ is the discretized frequency increment. Twenty modes were used, which is sufficient to avoid the effects of bath nonergodicity over the duration of the simulations. In

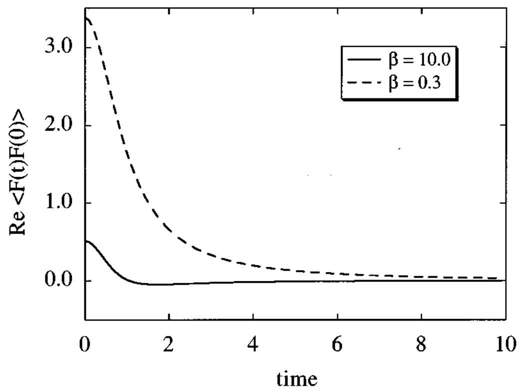

FIG. 2. A comparison of the real part of the force–force correlation function for an Ohmic Gaussian bath at $\beta=0.3$ and $\beta=10.0$.

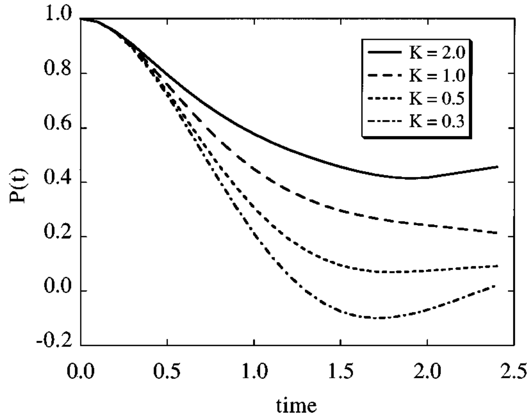

FIG. 4. A plot of $P(t)$ for the spin-boson model [Eq. (3.1)] at $\beta=0.3$ for several Kondo constants ranging from $K=0.3$ to $K=2.0$.

the present application, the spectral density was taken to be Ohmic with an exponential cutoff ω_c, given by

$$J(\omega)=\frac{\pi\hbar K}{2}\,\omega e^{-\omega/\omega_c}, \tag{3.5}$$

where K is the Kondo constant.[28] To demonstrate the temperature dependence of the bath forces, the real part of the force–force correlation function for the Ohmic bath with $\omega_c=1.0$ and $K=1.0$ is plotted in Fig. 2, where the solid curve corresponds to $\beta=10.0$ and the dashed curve corresponds to $\beta=0.3$. It is obvious that the effect of dissipation at high temperature is much stronger than that at low temperature.

The spin dynamics was simulated for different friction strengths as specified by the Kondo constant, and the population difference $P(t)$ is plotted as a function of time for $\beta=10.0$ in Fig. 3 and for $\beta=0.3$ in Fig. 4. At low friction, the quantum coherence is preserved, though the dissipation reduces the amplitude of the oscillations. As the strength of friction is increased, the spin dynamics exhibits a transition from coherent to incoherent behavior, which in some sense resembles the transition from the underdamped to overdamped behavior of a dissipative harmonic oscillator. This transition happens at about $K=0.5$, after which the dynamics becomes an exponential decay instead of damped oscillations. Since the purpose of using the model here is to demonstrate an application of the new algorithm, we will not discuss further the physical implications and theoretical predictions of the spin-boson model.[28]

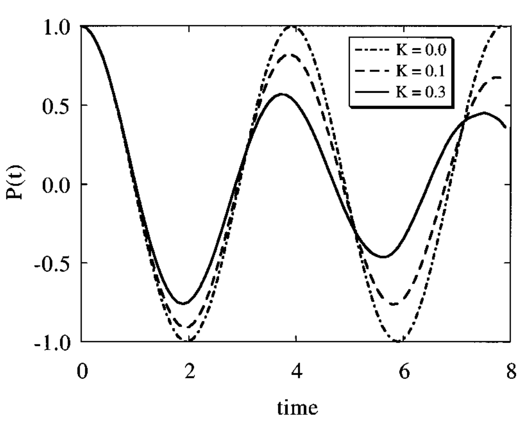

FIG. 3. A plot of $P(t)$ for the spin-boson model [Eq. (3.1)] at $\beta=10.0$ for several Kondo constants ranging from $K=0.0$ to $K=0.3$.

B. Dissipative quantum oscillator

In this section, the new algorithm will be used to study a type of system–bath Hamiltonian which models the vibrational relaxation of a solute oscillator in the condensed phase, i.e., the dissipative nonlinear quantum oscillator. This study is also intended to test the accuracy of the CMD method.[8–11] For undamped one-dimensional nonlinear oscillators at very low temperature, the CMD time correlation function may under certain conditions dephase somewhat faster than the exact quantum result. This behavior arises because the CMD initial conditions are sampled from a continuous Boltzmann-type centroid momentum distribution, whereas the exact quantum dynamics involves only the two lowest-lying states at low temperature. Essentially, any quasiclassical dynamical approximation is susceptible to difficulties in describing such "perfect" low temperature quantum coherence accurately, though CMD appears to capture the major quantum effects. It is important to note, however, that since most *real* quantum systems of interest are coupled to a surrounding medium, their dynamics is dissipative. In the condensed phase, this coupling usually dominates the dephasing and damping behavior. Under this circumstance, the ability of CMD to accurately describe the dynamics of many-body systems should be significantly enhanced. Here we investigate the damped quantum dynamics of a dissipative nonlinear quantum oscillator in order to demonstrate the implementation of the new algorithm and to better justify the use of CMD for many-body systems, such as liquid hydrogen,[12] proton transport,[13] liquid water,[14] etc.

In the CMD method,[8–11] it is argued that the quantum position or velocity correlation function can be related to a classical-like time correlation function for the centroid variable, where the centroid trajectories are generated by the classical-like equations of motion

$$m\ddot{q}_c(t)=F_c(q_c). \tag{3.6}$$

Here, the centroid force on the right-hand side of Eq. (3.6) is defined from the temperature-dependent quantum effective potential for the centroid variable, and a one-dimensional notation has been adopted for simplicity. Explicitly, the quantum mechanical centroid potential of mean force is given by

$$F_c(q_c)=-\frac{\int\cdots\int\mathscr{D}q(\tau)\,\delta(q_c-q_0)V'[q(0)]\exp\{-S[q(\tau)]/\hbar\}}{\int\cdots\int\mathscr{D}q(\tau)\,\delta(q_c-q_0)\exp\{-S[q(\tau)]/\hbar\}}, \tag{3.7}$$

where $S[q(\tau)]$ is the imaginary time action functional, and the centroid variable is defined as

$$q_0=\frac{1}{\hbar\beta}\int_0^{\hbar\beta}d\tau\, q(\tau). \tag{3.8}$$

The resulting centroid position correlation function is defined by

$$C^*(t)=\langle q_c(t)q_c(0)\rangle_{\rho_c}, \tag{3.9}$$

where the notation $\langle\cdots\rangle_{\rho_c}$ denotes an averaging over initial conditions with the phase space centroid density. It can be shown[10] that $C^*(t)$ is an approximation to the Kubo transformed position correlation function. In turn, this relates to the position correlation function through the Fourier transform relationship

$$\tilde{C}(\omega)=(\hbar\beta\omega/2)[\coth(\hbar\beta\omega/2)+1]\tilde{C}^*(\omega), \tag{3.10}$$

where $\tilde{C}(\omega)$ and $\tilde{C}^*(\omega)$ are the Fourier transforms of the quantum position and centroid position correlation functions, respectively. Because of its simplicity and stability, CMD has a wide appeal for large-scale simulations of many-body systems. Yet, since the method is approximate it is important that CMD continues to be rigorously examined through a comparison with exact numerical or experimental results for nontrivial systems as they become available. Indeed, the algorithm developed in this paper makes it possible to carry out such a comparison for systems described by Gaussian baths.

In accord with the CMD formulation, the centroid equations of motion for the system–bath Hamiltonian [Eq. (3.14)] can be reduced to a generalized Langevin equation (GLE) for the system centroid trajectory $q_c(t)$, namely,

$$m\ddot{q}_c(t)-F_c[q_c(t)]+\int_0^t dt'\,\eta(t-t')\dot{q}_c(t')=F(t), \tag{3.11}$$

where $F(t)$ is the random force on the system centroid from the bath and $\eta(t)$ is the dynamical friction kernel for the centroid motion defined in a similar fashion to Eq. (1.3). Here, the centroid force $F_c(q_c)$ is defined as in Eq. (3.7), but it involves an additional term in the imaginary time action resulting from the bath path integration, i.e.,

$$S[q(\tau)]=\int_0^{\hbar\beta}d\tau\left\{\frac{m}{2}\,\dot{q}(\tau)^2+V[q(\tau)]\right\}+\hbar\beta m\sum_{n=1}^{\infty}\Omega_n\hat{\eta}(\Omega_n)|a_n|^2, \tag{3.12}$$

where $\Omega_n=2\pi n/\hbar\beta$ and $\hat{\eta}(s)$ is defined by

$$\hat{\eta}(s)=\sum_{i=1}^{N}\frac{c_i^2}{m_i\omega_i^2}\,\frac{s}{s^2+\omega_i^2}. \tag{3.13}$$

The latter quantity is the Laplace transform of the dynamical friction kernel $\eta(t)$.

The system–bath Hamiltonian employed in the study described in this subsection is given by

$$H=\frac{p^2}{2m}+V(q)+\sum_{i=1}^{N}\left[\frac{p_i^2}{2m_i}+\frac{1}{2}\,m_i\omega_i^2\left(x_i-\frac{c_i}{m_i\omega_i^2}\,q\right)^2\right], \tag{3.14}$$

where the system potential $V(q)$ is given by

$$V(q)=\tfrac{1}{2}\,m\omega^2q^2+\tfrac{1}{4}\,mgq^4. \tag{3.15}$$

The parameters were chosen to be $m=1.0$, $\omega=1.0$, $g=1.0$, and $\beta=10.0$. The spectral density of the bath was taken to have the form of Ohmic friction, defined by Eq. (3.5), with a cutoff frequency of $\omega_c=1.0$.

Using a harmonic basis set, one can find the eigenstates of the system. Since only a few states are populated at low temperature, a finite basis set which diagonalizes the system Hamiltonian can be used to propagate the system under the influence of the bath. As such, the Hamiltonian becomes

$$H=\sum_{\mu=1}^{n}|\mu\rangle\epsilon_\mu\langle\mu|+\sum_{i=1}^{N}\frac{p_i^2}{2m_i}+\frac{1}{2}\,m_i\omega_i^2\left(x_i-\frac{c_i}{m_i\omega_i^2}\,\hat{q}\right)^2, \tag{3.16}$$

where the operator $\hat{q}$ is represented in the system basis as

$$\hat{q}=\sum_{\mu=1}^{n}\sum_{\nu=1}^{n}|\mu\rangle\langle\mu|\hat{q}|\nu\rangle\langle\nu|. \tag{3.17}$$

The cutoff of the system basis was chosen to be $n=4$ in the simulations. The dynamical quantity of interest in this case is the position–position correlation function of the system evolving under the influence of the bath. This time correlation function exhibits the dissipative effects arising from the vibrational relaxation of the system. The Ohmic bath was represented by twenty discretized harmonic oscillators with frequencies ranging from $\omega_1=\Delta\omega$ to $\omega_N=10.0\omega_c$, and 10^5 independent bath configurations were generated to Gaussian average the propagation of the system.

The calculation of the centroid force in the CMD simulation of the dissipative quantum oscillator was carried out approximately using the optimized quadratic reference potential which can be derived from a variational theory[43,44] or a diagrammatic analysis.[45] For the Hamiltonian in Eq. (3.14), the latter analysis leads to an expression for the system centroid-dependent effective harmonic frequency, given by

$$m\omega_c^2=\langle V''(q_c+\tilde{q})\rangle_\alpha = \frac{1}{\sqrt{2\pi\alpha_c}}\int d\tilde{q}V(q_c+\tilde{q})\exp(-\tilde{q}^2/2\alpha_c), \tag{3.18}$$

where the Gaussian width is given by

$$\alpha_c=\frac{2}{m\beta}\sum_{n=1}^{\infty}\frac{1}{\Omega_n^2+\omega_c^2+\Omega_n\hat{\eta}(\Omega_n)}. \tag{3.19}$$

The same treatment has been used previously to help formulate a variational theory[46] for the prefactor in path integral quantum transition state theory.[47,48] The self-consistent solution to the above transcendental equation yields an optimized harmonic reference potential with frequency ω_c and Gaussian width α_c. Consequently, the centroid force under the optimized quadratic approximation is given by

$$F_c(q_c)=\langle F(q_c+\tilde{q})\rangle_\alpha = -\frac{1}{\sqrt{2\pi\alpha_c}}\int d\tilde{q}V'(q_c+\tilde{q})\exp(-\tilde{q}^2/2\alpha_c). \tag{3.20}$$

For the present application, the centroid force in this approximation was calculated for 10^3 points on a one-dimensional grid and stored in an array. In order to make a rigorous comparison with the exact quantum calculation through the Gaussian force method, the bath friction kernel was represented by the same discrete set of harmonic oscillators. Therefore, any discrepancy between the CMD result and the exact result arises from the approximate nature of CMD. The CMD equations of motion were integrated with a time step of 0.1, and 10^5 trajectories were averaged to yield the centroid position correlation function, which was then converted to the real part of the quantum position correlation function via the Fourier relation in Eq. (3.10).

The real part of the position correlation function is shown for $K=0$ in Fig. 5, $K=0.1$ in Fig. 6, and $K=0.2$ in Fig. 7. The CMD results (solid curves) are compared in each figure with the exact results computed by the method introduced in this paper. For this low temperature system, the frictionless vibrational motion is completely coherent since only the two lowest-lying states are involved in the dynamics. The CMD result in Fig. 5 exhibits coherence until a relatively long time, at which point it starts to decay because of the unphysical dephasing introduced by the quasiclassical CMD momentum distribution. However, when the quantum system is coupled to the bath, the dissipation damps the quantum coherence and the position correlation function decays much faster than the nondissipative correlation function, depending of course on the strength of the dissipation. It can easily be seen from Figs. 6 and 7 that CMD then predicts the dissipative vibrational dephasing quite accurately in comparison with the exact results. It is also clear from these results that the physical vibrational dephasing comes into effect well before the unphysical long-time dephasing inherent in the CMD approximation. This result therefore supports the argument that CMD is an algorithm which can be reliably used for quantum systems in most condensed phase systems. For example, CMD has recently been found to give remarkably accurate agreement with experiment for the self-diffusion of liquid para-hydrogen.[12,15]

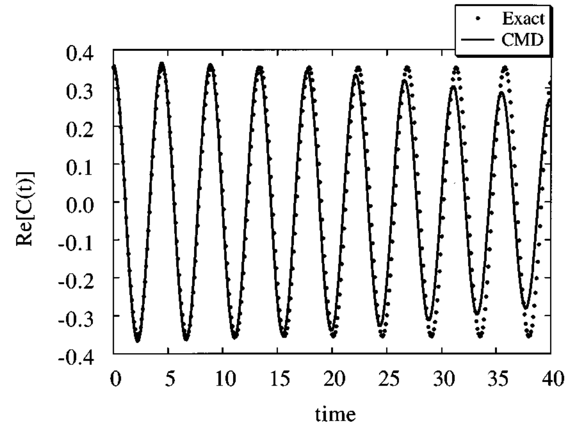

FIG. 5. A plot of the real time position correlation function at $\beta=10$ for the quartic potential described by Eq. (3.15). The solid line is the CMD result, while the solid circles are the numerically exact results obtained through the Gaussian averaging method.

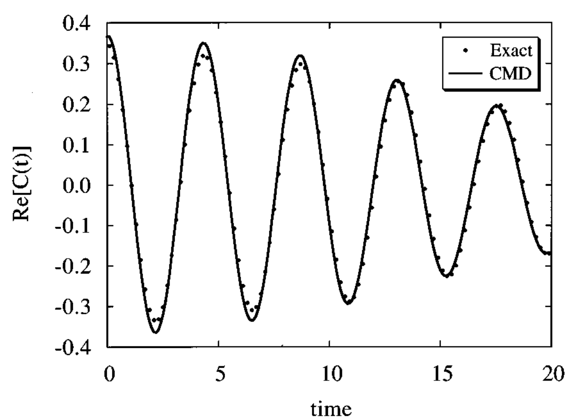

FIG. 6. A plot of the real time position correlation function at $\beta=10$ for the quartic potential described by Eq. (3.15) coupled to an Ohmic Gaussian bath with $K=0.1$. The solid line is the CMD result, while the solid circles are the numerically exact results obtained through the Gaussian averaging method.

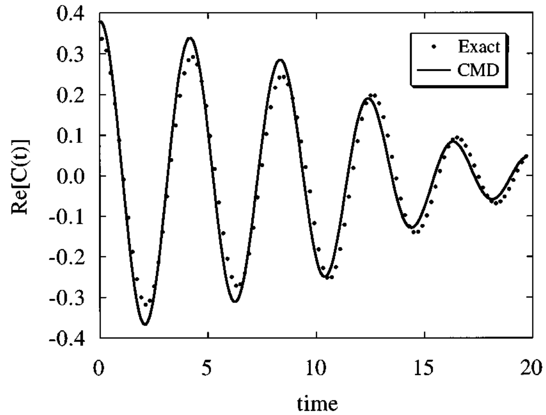

FIG. 7. A plot of the real time position correlation function at $\beta=10$ for the quartic potential described by Eq. (3.15) coupled to an Ohmic Gaussian bath with $K=0.2$. The solid line is the CMD result, while the solid circles are the numerically exact results obtained through the Gaussian averaging method.

IV. CONCLUDING REMARKS

In this paper, a simple and flexible method has been developed to sample the quantum fluctuating force in systems described by a Gaussian bath. It was shown by the examples presented in the last section that this algorithm is both accurate and efficient for such problems. This method also provides an alternative to numerical approaches based on the influence functional.[1] The numerical implementation of the influence functional approach introduces a cutoff in the number of discretized time slices, whereas the direct sampling of the Gaussian force introduces a cutoff in the number of discretized bath frequencies. Consequently, the former approach is preferable if the correlation time of the influence functional is short, while the latter approach is advantageous if the width of the bath spectral density is narrow or relatively localized around certain frequencies. For systems where the two approaches are equally effective, then the present algorithm seems to be more straightforward and flexible to implement. For example, since the quantum system evolves according to the Shrödinger equation under the influence of a time dependent Gaussian force, our algorithm can be combined with any exact or approximate numerical scheme for quantum propagation such as basis set methods, wave packet dynamics, semiclassical dynamics, path integration, or curve crossing methods. Some of these methods do not seem as compatible with the influence functional approach because of its convolution of the time integration. With the present methodology and other developments, we should be able to study a wide range of "system–bath" quantum dynamical processes such as two- and multistate electron transfer, quantum tunneling, photoexcitation and photodissociation, vibrational relaxation, quantum activated dynamics, etc.

Another appealing feature of the present method is that it can be readily generalized to simulate the influence of a bath having an arbitrary time-dependent Gaussian distribution instead of the equilibrium Boltzmann distribution. Such situations arise, for example, in ultrafast laser experiments where the "bath" (e.g., electron–hole pairs in a metal) is excited by the laser pulse and rapidly "equilibrates" to an effectively higher temperature Boltzmann distribution. The time-dependent relaxation of the bath temperature is then governed by a phenomenological heat transport equation. To carry out a simulation of a quantum "system" (e.g., an adsorbate vibration) in such an environment, the imaginary time bath paths $x_\beta(\tau)$ are treated differently from the forward and backward real time paths. The two terminal points x_1 and x_2 can be generated directly according to the instantaneous bath distribution function by Monte Carlo methods; the third terminal point x_3 is next sampled from an imaginary Gaussian matrix which connects to the points x_1 and x_2; the forward and backward real time paths are then given according to Eq. (2.14), but the imaginary time bath paths are sampled from the imaginary time equivalent to Eq. (2.14), again for the time-dependent bath temperature. In general, as long as the real time dynamics is adequately described by the linearized system–bath Hamiltonian, the present method is applicable to nonequilibrium situations, as the statistical distribution can be sampled directly by Monte Carlo methods.

As a final point, we note that a given spectral density has been assumed throughout this paper. For a realistic system, it remains an interesting question how best to obtain a spectral density which describes the linear response of a *quantum* bath to the motion of the system. The standard procedure is to calculate the *classical* force–force correlation function projected along the system coordinate, from which the classical friction kernel $\eta(t)$ can be determined through the fluctuation-dissipation relation in Eq. (1.5). In turn, the spectral density for the effective classical Gaussian bath can be extracted by an inverse cosine transform [cf. Eqs. (1.3) and (1.4)]. It is then *assumed* that the spectral density for the quantum effective Gaussian bath is *the same* as for the classical limit. While this approach is certainly correct for a rigorously harmonic bath, it is hard to know whether it is valid for real systems. An alternative picture[49] based on variational theory[50] has been recently developed by the present authors. The basic approach is to determine the best effective harmonic representation of the bath Hamiltonian according to the optimized quadratic approximation (OQA).[50] This specifies a set of optimal normal modes[49] corresponding to the different inherent structures of the bath. A phenomenological decay function is next introduced to describe the average transition rate between the different sets of optimized normal modes, thus leading to the concept of the damped normal mode (DNM).[49] The damping constant can be chosen so certain known properties of the bath are exactly reproduced (e.g., the self-diffusion constant for a pure liquid). By virtue of this approach, it was found that a classical dynamical friction along a solute bond can be predicted which agrees remarkably well with exact MD simulation. Since the DNM theory is readily generalized to quantum systems, this theory provides a direct route to specify the spectral density of an effective Gaussian quantum bath. Obviously, for such systems the exact quantum dynamical calculation of the force–force correlation function is not feasible, so the DNM method may in fact be the method of choice. This issue, as well as applications of the theory presented in the present paper, will be the topic of future research.

ACKNOWLEDGMENTS

This research was supported by the National Science Foundation (CHE-9158079) and (CHE-9410608) and by the Office of Naval Research. G.A.V. is a recipient of a National Science Foundation Presidential Young Investigator Award, a David and Lucile Packard Fellowship in Science and Engineering, an Alfred P. Sloan Foundation Research Fellowship, and a Camille Dreyfus Teacher–Scholar Award. L. Ungar received partial support through a Packard Fellowship to N. F. Scherer.

APPENDIX: DIAGONALIZATION OF THE S MATRIX

Given the action in Eq. (2.6), one can express the matrix $\mathbf{S}/\hbar$ as

$$\mathbf{S}/\hbar=\begin{pmatrix} A-iC & -B & iD \\ -B & A+iC & -iD \\ iD & -iD & 0 \end{pmatrix}, \tag{A1}$$

where the elements of the matrix have the following values: $A=m\omega/\hbar\tanh(\hbar\beta\omega)$, $B=m\omega/\hbar\sinh(\hbar\beta\omega)$, $C=m\omega/\hbar\tan(\omega t)$, and $D=m\omega/\hbar\sin(\omega t)$. The secular solution of a three dimensional matrix results in a cubic equation which can be solved analytically. However, since the third diagonal element in Eq. (A1) is zero, one can first diagonalize the two dimensional submatrix formed by the first two columns and rows, and then eliminate the bilinear terms on the third column and row by completing the squares.

This procedure yields for the diagonal elements of $\{\lambda\}$,

$$\lambda_1=A+\Delta, \tag{A2}$$

$$\lambda_2=A-\Delta, \tag{A3}$$

and

$$\lambda_3=\frac{2D^2(A-B)}{A^2-\Delta^2}, \tag{A4}$$

where $\Delta=\sqrt{B^2-C^2}$. Substituting the values of the parameters, we find a rather simple expression for λ_3, that is

$$\lambda_3=2(A-B)=\frac{2m\omega}{\hbar}\tanh(\hbar\omega\beta/2). \tag{A5}$$

The transformation matrix $\mathbf{U}$ is given by (again by using $A^2-\Delta^2=D^2$),

$$\mathbf{U}=\begin{pmatrix} \frac{\sqrt{\Delta-iC}}{\sqrt{2\Delta}} & \frac{\sqrt{\Delta+iC}}{\sqrt{2\Delta}} & \frac{1}{D}[C-i(A-B)] \\ -\frac{\sqrt{\Delta+iC}}{\sqrt{2\Delta}} & \frac{\sqrt{\Delta-iC}}{\sqrt{2\Delta}} & \frac{1}{D}[C+i(A-B)] \\ 0 & 0 & 1 \end{pmatrix}. \tag{A6}$$

The above results can be verified by calculating various correlation functions of the linear harmonic oscillator.

[1] R. P. Feynman and A. R. Hibbs, *Quantum Mechanics and Path Integrals* (McGraw–Hill, New York, 1965).
[2] B. J. Berne, J. Stat. Phys. **43**, 911 (1986).
[3] L. S. Schulman, *Techniques and Applications of Path Integration* (Wiley, New York, 1986).
[4] J. D. Doll and J. E. Gubernatis, *Quantum Simulations of Condensed Matter Phenomena* (World Scientific, Singapore, 1990).
[5] D. Chandler, in *Liquides, Cristallisation et Transition Vitreuse Les Houches, Session LI*, edited by D. Levesque, J. Hansen, and J. Zinn-Justin (Elsevier, New York, 1991).
[6] M. S. Swanson, *Path Integrals and Quantum Processes* (Academic, San Diego, 1992).
[7] M. F. Herman, Annu. Rev. Phys. Chem. **45**, 83 (1994).
[8] J. Cao and G. A. Voth, J. Chem. Phys. **99**, 10 070 (1993).
[9] J. Cao and G. A. Voth, J. Chem. Phys. **100**, 5106 (1994).
[10] J. Cao and G. A. Voth, J. Chem. Phys. **101**, 6157 (1994).
[11] J. Cao and G. A. Voth, J. Chem. Phys. **101**, 6168 (1994).
[12] J. Cao and G. Martyna, J. Chem. Phys. **104**, 2028 (1996).
[13] J. Lobaugh and G. A. Voth, J. Chem. Phys. **104**, (1996). This paper describes a CMD simulation of excess proton transport in liquid water.
[14] J. Lobaugh, M. Pavese, and G. A. Voth, J. Chem. Phys. (to be published). This paper describes a CMD simulation of quantum water.
[15] M. Pavese and G. A. Voth, Chem. Phys. Lett. (in press). This paper describes a CMD simulation of self-diffusion in liquid para-hydrogen.
[16] G. A. Voth, Adv. Chem. Phys. (in press).
[17] R. Zwanzig, J. Stat. Phys. **9**, 215 (1973).
[18] A. O. Caldeira and A. J. Leggett, Ann. Phys. (NY) **149**, 374 (1983).
[19] A. Schmid, J. Low. Temp. Phys. **49**, 5 (1982).
[20] E. Pollak, J. Chem. Phys. **85**, 865 (1986).
[21] R. P. Feynman, *Statistical Mechanics* (Addison–Wesley, MA, 1972), Chap. 3.
[22] R. Coalson, J. Chem. Phys. **86**, 995 (1987).
[23] R. Coalson, J. Chem. Phys. **94**, 1108 (1991).
[24] C. H. Mak and D. Chandler, Phys. Rev. A **41**, 5709 (1990).
[25] C. H. Mak and D. Chandler, Phys. Rev. A **44**, 2352 (1991).
[26] R. Egger and C. H. Mak, J. Chem. Phys. **99**, 2541 (1993).
[27] R. Egger, C. H. Mak, and U. Weiss, J. Chem. Phys. **100**, 2651 (1994).
[28] A. J. Leggett, S. Chakravarty, A. T. Dorsey, M. P. A. Fisher, A. Garg, and W. Zwerger, Rev. Mod. Phys. **59**, 1 (1987).
[29] D. Makarov and N. Makri, Phys. Rev. A **48**, 3626 (1993).
[30] D. Makarov and N. Makri, Chem. Phys. Lett. **221**, 482 (1994).
[31] M. Topaler and N. Makri, J. Chem. Phys. **101**, 7500 (1994).
[32] N. Makri and D. E. Makarov, J. Chem. Phys. **102**, 4600 (1995).
[33] N. Makri and D. E. Makarov, J. Chem. Phys. **102**, 4611 (1995).
[34] D. Thirumalai, E. J. Bruskin, and B. J. Berne, J. Chem. Phys. **79**, 5063 (1983).
[35] R. Kosloff, J. Phys. Chem. **92**, 2087 (1988).
[36] E. J. Heller, J. Chem. Phys. **62**, 1544 (1975).
[37] G. Campolieti and P. Brumer, Phys. Rev. **50**, 997 (1994).
[38] J. Cao and G. A. Voth, J. Chem. Phys. **104**, 273 (1996).
[39] J. Doll, R. Coalson, and D. Freeman, J. Chem. Phys. **87**, 1641 (1987).
[40] J. Chang and W. Miller, J. Chem. Phys. **87**, 1648 (1987).
[41] N. Makri and W. H. Miller, J. Chem. Phys. **89**, 2170 (1988).
[42] M. Suzuki, Proc. Jpn. Acad. **69**, 161 (1993).
[43] R. Giachetti and V. Tognetti, Phys. Rev. Lett. **55**, 912 (1985).
[44] R. P. Feynman and H. Kleinert, Phys. Rev. A **34**, 5080 (1986).
[45] J. Cao and G. A. Voth, J. Chem. Phys. **100**, 5093 (1994).
[46] G. A. Voth, Chem. Phys. Lett. **270**, 289 (1990).
[47] G. A. Voth, D. Chandler, and W. H. Miller, J. Chem. Phys. **91**, 7749 (1989).
[48] G. A. Voth, J. Phys. Chem. **97**, 8365 (1993). For a review of path integral quantum transition state theory, see this paper.
[49] J. Cao and G. A. Voth, J. Chem. Phys. **103**, 4211 (1995).
[50] J. Cao and G. A. Voth, J. Chem. Phys. **102**, 3337 (1995).